Rate Dependent Constitutive Equations of Cyclic Softening

J. S. Mshana

Lecturer, Department of Mechanical Engineering, University of Dar-es-Salaam, Tanzania, currently on study leave for Ph.D. studies, Department of Mechanical Engineering, University of Ottawa, 770 King Edward Ave., Ottawa, Ont., Canada K1N 6N5

A. S. Krausz

Department of Mechanical Engineering, University of Ottawa, Ottawa, Ont., Canada

Z. Naturforsch. **40 a**, 653–665 (1985); received December 8, 1984

Constitutive equations of cyclic strain and stress softening for materials with low internal stress levels are derived from the rate theory. The study shows that over the high stress and low temperature range where the description of plastic flow in cyclic softening can be approximated with activation over a single energy barrier, cyclic strain softening is well related to stress relaxation process while cyclic stress softening is related to creep process. The material structural characteristics for cyclic strain softening, cyclic stress softening and stress relaxation are identical. Subsequently, it is shown that cyclic stress and strain softening within the high stress and low temperature range can be evaluated from the constitutive equations using the material structural characteristics measured from a simple stress relaxation test.

1. Introduction

1.1 Gross cyclic deformation behavior

The fracture of structural metals subjected to cyclic plastic loading is critical in the design of steam and gas turbines, jet engines, nuclear reactors, etc. To understand the fracture process, the mechanisms of cyclic plastic deformation were studied from metallurgical standpoint in many papers, e.g. [1–3], to name just a few. The interest of these studies was in the mechanism of slip, dislocation movements, and other changes in the metallurgical structure. However, the exploration of the gross deformation behavior, another aspect of cyclic plastic loading, has not received a great deal of attention [1–6]. These efforts are characterized by the systematic study of the deformation behavior through the measurement of stress and displacement (strain). The ultimate objective of these investigations is the formulation of constitutive equations, the mathematical description of the material behavior.

Despite these explorations, neither material science nor the continuum theory of plasticity has advanced to the stage of being able to predict the macroscopic cyclic stress-strain behavior of real materials. In addition, machine components are often subjected to complex cyclic loading regimes. Consequently, the formulation of realistic constitutive equations for cyclic plastic straining is a formidable task. In the following, the constitutive equations of thermally activated cyclic plastic flow for the case where the material undergoes cyclic softening will be derived from rate theory (usually called transition state theory, or activated complex theory, or absolute rate theory). It will also be shown that the material structural characteristics determined from a simple stress relaxation test can be used to predict the cyclic softening behavior using the constitutive equations.

Reprint requests to Herrn Prof. A. S. Krausz, Dept. of Mechanical Engineering, University of Ottawa, 770 King Edward Ave., Ottawa, Ont., Canada K1N 6N5

1.2. Thermally activated cyclic softening

During cyclic loading of a machine component the total strain ε is the sum of two components: the elastic strain, ε_e, and the plastic strain, ε_p. The elastic strain is fully reversible and cannot cause any damage. It is the plastic deformation which causes cumulative and irreversible changes in the material substructure: in the dislocation substructure [2, 3] and in broken bonds such as microcracks and vacancies and [7], therefore, only the cyclic plastic deformation is considered as the most decisive phenomenon in the fracture process.

Considerable efforts were made to interpret the behavior exhibited by many materials under a

0340-4811 / 85 / 0700-0653 $ 01.30/0. – Please order a reprint rather than making your own copy.

variety of different uniaxial plastic deformation processes and to represent the behavior by essentially empirical expressions [1–10]. Usually a vast amount of experimental observation is needed before fairly general conclusions can be reached. Constitutive equations obtained from this type of phenomenological models have limited applications since they cannot be used outside of their actually tested range. In addition, the empirical constitutive equations cannot, as a rule, be identified with the basic material structural characteristics and, in most cases, they cannot represent the effect of the important service and manufacturing parameter – the temperature.

Plastic deformation is generelly produced by the motion of dislocations under the drive of the applied shear stress [3, 7, 11, 14]. In most cases, it is rate dependent (and, therefore, temperature dependent); that is, thermally activated. It was shown by Krausz and Eyring [11] that thermally activated plastic flow and chemical reactions are essentially identical processes, since both are solely the consequence of breaking and establishing of atomic bonds. Because of this fundamental general fact, plastic deformation was considered as a chemical reaction in which the composition remains unchanged, but the atomic configuration changes. The rigorous physical foundation of absolute rate theory was established by Eyring in 1936 [12] and it was incorporated into dislocation theory by Orowan [13]. Consequently, the constitutive equation for thermally activated plastic flow was expressed as [3, 7, 11, 13, 14]

$$\dot{\varepsilon}_p = \left(\frac{1}{M}\right) b\, \varrho_m\, \bar{v} = \left(\frac{1}{M}\right) b\, \varrho_m\, \bar{l}\, \not{k} \tag{1a}$$

and in simple kinetics, as

$$\dot{\varepsilon}_p = \left(\frac{1}{M}\right) b\, \varrho_m\, \bar{l}(\not{k}_f - \not{k}_b), \tag{1b}$$

where $\dot{\varepsilon}_p$ is the plastic tensile strain rate, M is the Taylor orientation factor relating the tensile stress σ and tensile strain ε to the shear stress $\tau (= \sigma/M)$ and shear strain γ $(= M\varepsilon)$ resolved in the rate-controlling slip system, b is the Burger's vector, ϱ_m is the mobile dislocation density, $\bar{l}$ is the distance travelled by the dislocation between obstacles, $\bar{v}$ is the average dislocation velocity and $\not{k}$ is the overall rate constant which represents the simplest possible combination of the fundamental rate constants $\not{k}_f$ and $\not{k}_b$ which were derived from statistical mechanics as [11]

$$\not{k}_f = \frac{kT}{h} \exp -\frac{\Delta G_f}{kT}, \quad \not{k}_b = \frac{kT}{h} \exp -\frac{\Delta G_b}{kT}. \tag{2}$$

In (2), k is the Boltzmann constant, T is the temperature, h is the Planck's constant, ΔG is the apparent free energy and the subscripts f and b refer to the forward and backward activations, respectively over a single energy barrier. The apparent free energy is the energy needed from the thermal fluctuations of the atoms to cause dislocation motion, and it is expressed as [11]

$$\Delta G_f = \Delta G_f^* - W_f(\tau), \quad \Delta G_b = \Delta G_b^* + W_b(\tau), \tag{3}$$

where ΔG^* is the free energy of activation and is equal to the chemical, bond energy associated with the atoms that take part in the dislocation movement; $W(\tau)$ is the work contributed by the shear stress τ which causes the plastic flow. Thermally activated plastic deformation is often controlled by a system of energy barriers which may form either a parallel system, a consecutive system, or a combination of these two types. Hence, to obtain a physically meaningful description of the experimental results, a kinetics analysis [11, 14, 15] has to be carried out first, that will give the appropriate system of the energy barriers. Then, as it is practiced in chemical kinetics studies, the combination of the individual rate constants or the overall rate constant $\not{k}$ can be determined. The required activation parameters are determined from the evaluation of the experimental results and from the testing conditions. It was established by Krausz and Eyring [11] and also by Krausz and Faucher [14, 15] that (1a) and (1b) lead to very good description of the behavior of many materials under a variety of different uniaxial deformation processes and that it can often provide a mathematically even simpler expression than the phenomenological models.

In our previous papers [16, 17] it was considered that plastic flow during cyclic strain softening is a thermally activated process and the constitutive equation describing the shear stress in function of time during cyclic strain softening was derived. It was shown that cyclic strain softening is associated with stress relaxation and that the two phenomena are parallel over a high stress and low temperature range where thermally activated plastic flow in the two processes can be approximated with activation over a single energy barrier. The present paper

reviews and extends this work to analyze the constitutive equation of cyclic softening for an alternative cyclic loading: load controlled cyclic loading.

2. Discussion

2.1. Constitutive equation of cyclic strain softening

2.1.1. Summary

The constitutive equation of cyclic strain softening for materials with low (or negligible) internal stress levels was derived in our previous paper [16]. The study showed that cyclic strain softening is a rate phenomenon, strongly dependent on the temperature and loading rate, and that it can be tested in stress relaxation. Within the high stress and low temperature zone the material structural characteristics were identical in both processes leading to the recommendation that stress relaxation can be employed to measure quantitatively the microstructural characteristics for the understanding of cyclic strain softening process. In the present paper, the hysteresis loops that were calculated by using the constitutive equation for which the microstructural characteristic values were measured in a simple stress relaxation test, are compared with experimental data. The derivation of the constitutive equation of cyclic strain softening is reviewed here so as to present a coherent analysis of the rate dependent constitutive equation of cylic softening; both for strain and load controlled cyclic loading.

2.1.2. Elastic and plastic strain rates

During cyclic softening, the total strain $\varepsilon(t)$ is expressed as

$$\varepsilon(t) = \varepsilon_e + \varepsilon_p \tag{4}$$

or in time differential notation as

$$\dot{\varepsilon} = \dot{\varepsilon}_e + \dot{\varepsilon}_p . \tag{5}$$

The elastic strain is related to the shear stress as

$$\varepsilon_e = \frac{\sigma}{E} = \frac{M\tau}{E} , \tag{6}$$

where E is the combined elastic modulus describing the net elastic response of the test specimen and grip assembly. Consequently, the elastic strain rate is expressed as

$$\dot{\varepsilon}_e = \frac{\dot{\sigma}}{E} = \frac{M\dot{\tau}}{E} . \tag{7}$$

Cyclic softening, like other plastic deformation processes is time and temperature dependent and, therefore, thermally activated [7, 10, 11, 14, 15, 16]. In a specific stress and temperature range a single energy barrier may control the plastic flow. The plastic strain rate is then described by (1 b). Within this range the mechanical energy $W(\tau)$, that is, the work done by the effective shear stress τ_{eff} acting on the dislocation or flow unit is, in most cases, assumed to be a linear function of the effective shear stress [7, 11] thus

$$W(\tau) = V\tau_{eff} = V(\tau - \tau_i) \tag{8}$$

since $\tau_{eff} = \tau - \tau_i$, where τ is the applied shear stress, τ_i is the internal shear stress representing the resistance of the material to dislocation motion and V is the activation volume or the product of the area swept out by a dislocation during a thermally activated movement and the Burger's vector, b, of the dislocation. In the high stress and low temperature zone plastic flow is controlled by a single energy barrier and the rate of backward activation is much less than the rate of forward activation, i.e. $\lambda_f \gg \lambda_b$. Consequently, at high stress levels, it is satisfactory to represent the kinetics of the rate controlling system by activation in the forward direction only and over a single energy barrier, that is, $\lambda = \lambda_f$ [11]. Equation (1) then becomes

$$\dot{\varepsilon}_p = A_f \exp \frac{V_f(\tau - \tau_i)}{kT} , \tag{9}$$

where

$$A_f = \left(\frac{1}{M}\right) b\, \varrho_m\, \bar{l}\, \frac{kT}{h} \exp - \frac{\Delta G_f^*}{kT} .$$

It was found that in the high stress and low temperature range, (9) describes well the deformation behavior of many crystalline materials [3, 7, 10, 11, 14, 15].

2.1.3. Constitutive equation

The constitutive equation of cyclic strain softening was derived for the high stress and low temperature range. In this zone, the applied shear stress rate can be deduced from (9) as

$$\dot{\tau}\,|_T = \frac{kT}{V_f}\frac{1}{\dot{\varepsilon}_p}\frac{d\dot{\varepsilon}_p}{dt} - \frac{\tau_{eff}}{V_f}\frac{dV_f}{dt} - \frac{kT}{V_f}\frac{1}{A_f}\frac{dA_f}{dt} + \frac{d\tau_i}{dt} . \tag{10a}$$

However, it was established by Krausz and Eyring [11] that in the high stress and low temperature zone

the activation volume is independent of stress and time: no structural change. Also, the evaluation of experimental results for some materials with low internal stress levels [11, 16, 18, 19, 20] have shown that when the total strain amplitude is small, the components of the shear stress rate due to mobile dislocation density (and/or microstructure) changes and to the internal stress rate are negligible compared to the component due to the change of the plastic strain rate. Hence, the applied shear stress rate in the high stress and low temperature range and during cyclic strain softening of these materials can be approximated as

$$\dot{\tau}|_{\mathrm{T}} = \frac{kT}{V_{\mathrm{f}}} \frac{1}{\dot{\varepsilon}_{\mathrm{p}}} \frac{\mathrm{d}\dot{\varepsilon}_{\mathrm{p}}}{\mathrm{d}t} . \tag{10b}$$

While the above assumptions are physically reasonable, they are by no means necessary and should not be taken as restrictions on the validity of the theory. The combination of (5), (7), and (10) results in

$$\frac{MkT}{EV_{\mathrm{f}}} \frac{1}{\dot{\varepsilon}_{\mathrm{p}}} \frac{\mathrm{d}\dot{\varepsilon}_{\mathrm{p}}}{\mathrm{d}t} + \dot{\varepsilon}_{\mathrm{p}} = \dot{\varepsilon} . \tag{11}$$

The solution of (11) is [16, 21]

$$\dot{\varepsilon}_{\mathrm{p}} = \frac{A_{\mathrm{f}} \exp\left\{\frac{EV_{\mathrm{f}}}{2kT}\varepsilon(t)\right\}}{EA_{\mathrm{f}}\frac{V_{\mathrm{f}}}{2kT}\int_0^t \left\{\exp\frac{EV_{\mathrm{f}}\varepsilon(t)}{2kT}\right\}\mathrm{d}t + \exp\left\{\frac{V_{\mathrm{f}}}{2kT}(E\varepsilon_0 - 2\tau_0)\right\}} , \tag{12}*$$

where t is the deformation time, ε_0 is the initial total strain, τ_0 is the initial applied shear stress and the Taylor orientation factor M was assumed to be equal to 2 (an approximate value for most polycrystalline materials). The applied shear stress for the case where the total strain function is in form of a triangular wave (or $\varepsilon = \varepsilon_0 + \varepsilon_1(t)$ where $\varepsilon_1(t)$ is the cyclic strain as shown in Fig. 1) was evaluated as

$$\tau = \frac{E\varepsilon_1(t)}{2} + \tau_0 - \frac{kT}{V_{\mathrm{f}}} \ln \left| \frac{EA_{\mathrm{f}}V_{\mathrm{f}}}{2kT}\left(\exp\frac{V_{\mathrm{f}}\tau_0}{kT}\right) \cdot \int_0^t \left\{\exp\frac{EV_{\mathrm{f}}\varepsilon_1(t)}{2kT}\right\}\mathrm{d}t + 1\right| . \tag{13}$$

* In (12), the plastic strain rate becomes indeterminate at finite deformation time t when $\varepsilon, \dot{\varepsilon} \to \infty$. However, at high strain rates the velocity of dislocations is limited by the velocity of transverse sound waves in the material. Thermally activated dislocation movement ends – fades out – at strain rates several orders of magnitude below this [11, 14].

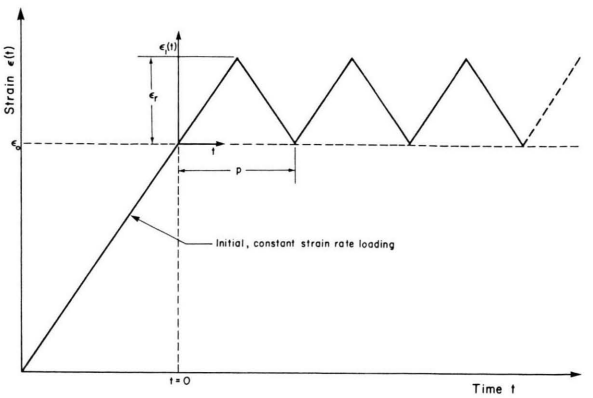

Fig. 1. A schematic representation of a triangular strain wave used in strain controlled fatigue tests. ε_{r} is the strain range, p is the period and $\varepsilon(t) = \varepsilon_0 + \varepsilon_1(t)$.

Stress relaxation is a special case of cyclic strain softening where $\varepsilon_1(t) \cong 0$. For this, (13) reduces to

$$\tau = \tau_0 - \frac{kT}{V_{\mathrm{f}}} \ln \left| \frac{EA_{\mathrm{f}}V_{\mathrm{f}}}{2kT}\left(\exp\frac{V_{\mathrm{f}}\tau_0}{kT}\right) t + 1\right| . \tag{14}$$

Over the temperature, stress, and time range where thermally activated flow in cyclic strain softening and stress relaxation can be approximated with activation over a single energy barrier, (14) was used to evaluate the material structural characteristics (the activation volume and the activation free energy) [16] for cyclic strain softening. Consequently, the shear stress-time response during cyclic strain softening can be calculated from (13) using the structural characteristics evaluated from stress relaxation.

2.2. *Constitutive equation of cyclic stress softening*

Cyclic stress softening, like cyclic strain softening, is a plastic deformation process. While cyclic stress softening is denoted by a cycle dependent increase in the absolute value of the strain under constant load amplitude, cyclic strain softening is defined as a cycle dependent decrease in the absolute value of the stress under constant strain amplitude. In the

simplest deformation kinetics where thermally activated plastic flow in cyclic stress softening can be approximated with activation over a single energy barrier, the plastic strain rate, as in Sect. 2.1, is expressed as

$$\dot{\varepsilon}_p = \left(\frac{1}{M}\right) b \varrho_m \frac{kT\bar{l}}{h} \exp - \frac{\Delta G_f^* - V_f \tau_{eff}}{kT}. \quad (15)$$

The mobile dislocation density, ϱ_m, is essentially an experimentally measurable quantity and is expressed in terms of the stress or strain. A widely used form was introduced by Johnston [22] i.e.

$$\varrho_m = \varrho_m^0 + B \varepsilon_p, \quad (16)$$

where ϱ_m^0 is the mobile dislocation density measured at the beginning of plastic flow and is thus an empirical parameter that represents the previous deformation (state of the structure) history. It is outside of the theory of deformation kinetics and of the theory used here: it is also a microstructural feature to be measured by the method given in this paper. The factor B is also measured by direct dislocation density observation and expresses the multiplication of dislocations in function of the strain. Equations (15) and (16) can be combined and rearranged as

$$\frac{d\varepsilon_p}{\varrho_m^0 + B\varepsilon_p} = A_f' \left(\exp \frac{V_f \tau_{eff}}{kT}\right) dt, \quad (17)$$

where $A_f' = A_f/\varrho_m$. For the purpose of the present discussion, we consider (as in Sect. 2.1.3) the cyclic deformation of materials with low internal stress levels. In this model, therefore, the applied stress is approximately equal to the effective stress. An extension for non-zero τ_i and increasing τ_i, that is,

$$\tau_i = \tau_i^0 + H \varepsilon_p,$$

where τ_i^0 is the internal stress at the beginning of the experiment and H is the work hardening coefficient will be presented elsewhere [23]. During load controlled cyclic loading, the applied shear stress is a periodic, random or complex function of time. Figure 2 shows a triangular load wave form often used for load cycling or fatigue experiments. The applied normal stress is of the form

$$\sigma = \sigma_0 + \sigma_1(t), \quad (18)$$

where σ_0 is the initial stress (load) at $t = 0$ and $\sigma_1(t)$ is the cyclic stress. It is defined for the first cycle, or any other cycle as

$$\sigma_1(t) = \begin{cases} \dfrac{2\sigma_r t}{p} & \text{when } 0 < t \leqq \dfrac{p}{2}, \\ \dfrac{2\sigma_r (p-t)}{p} & \text{when } \dfrac{p}{2} \leqq t \leqq p, \end{cases} \quad (19)$$

where p is the period and σ_r is the stress (or load amplitude) range. Again, in the high stress and low temperature range the activation volume is independent of stress and time. Substituting (18) and (19) into (17) and integrating (Appendix) we obtain

$$\frac{1}{B} \ln \left(1 + \frac{B}{\varrho^0} \varepsilon_p\right) = A_f' \frac{2kTt}{V_f} \left(\exp \frac{V_f \sigma_0}{2kT}\right) \left| \frac{\exp \dfrac{V_f \sigma_r}{2kT} - 1}{\sigma_r} \right|. \quad (20)$$

As in Sect. 2.1, the Taylor orientation factor M was assumed to be equal to 2. When the mobile dislocation density ϱ_m has reached a steady state value or when the dislocation multiplication coefficient B is very small so that

$$\frac{B}{\varrho_m^0} \varepsilon_p \ll 1 \quad (21)$$

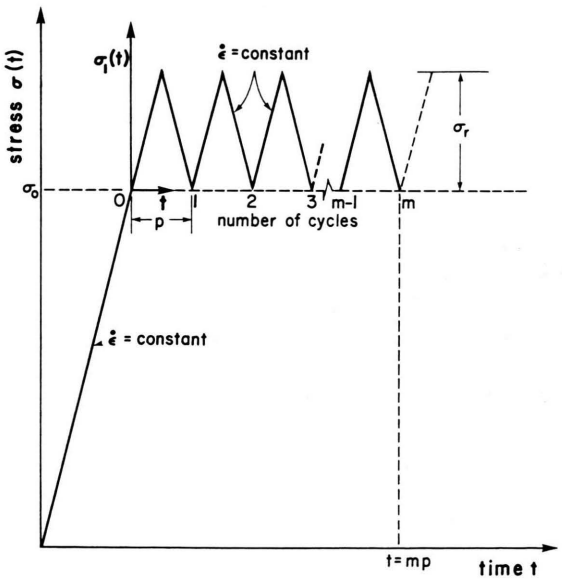

Fig. 2. A schematic representation of a triangular load wave form often used in load (stress) controlled cyclic loading experiments. σ_r is the stress range, p is the period and σ_0 is the initial stress.

then the integration of (17) leads to

$$\varepsilon_p = A_f \frac{2kT}{V_f}\left(\exp\frac{V_f\sigma_0}{2kT}\right) \cdot \left|\frac{\left(\exp\frac{V_f\sigma_r}{2kT}\right)-1}{\sigma_r}\right| t - \sigma_0/E + \varepsilon_0 . \quad (22)$$

That is, during constant load amplitude cyclic stress softening deformation process the plastic strain is proportional to the deformation time t. The total strain, ε, is then expressed as

$$\varepsilon = \frac{\sigma_1}{E} + \varepsilon_0 + A_f \frac{2kT}{V_f}\left(\exp\frac{V_f\sigma_0}{2kT}\right)\frac{\exp\frac{V_f\sigma_r}{2kT}-1}{\sigma_r} t. \quad (23)$$

In the limit when $\sigma_r \to 0$ or during creep deformation, (23) reduces to

$$\varepsilon = \varepsilon_0 + A_f\left(\exp\frac{V_f\sigma_0}{2kT}\right) t. \quad (24)$$

Consequently, the strain rate during steady state, secondary creep is expressed in function of the applied stress as

$$\dot{\varepsilon} = A_f \exp\frac{V_f\sigma}{2kT}, \quad (25)$$

where $\sigma = \sigma_0 = \text{constant}$.

The total strain is not proportional to $\ln t$ because $\tau_i = \text{constant}$: a measure of constant microstructure. The conclusion that follows from (23) and (24) is an important one: creep deformation process is a special case of cyclic stress softening. Consequently, it is anticipated that creep tests can be used to measure the constitutive parameters V_f and A_f that represents the microstructure which can then be used in the development of the constitutive equation of the more complicated cyclic stress softening process. Hence, over the temperature, stress and time range where thermally activated flow in cyclic stress softening and creep can be approximated with activation over a single energy barrier, (24) can be used to evaluate the constitutive parameters for the cyclic stress softening process. The total strain-time response during cyclic stress softening can then be calculated from (17) and (21).

3. Experimental Details

3.1. Material

The material under investigation was a commercial grade, near eutectoid Zn-Al superplastic alloy of nominal composition: Al 25 Wt%, Cu 5 Wt%, Mg 0.05 Wt%, Zn balance. The material was selected because, as determined in a previous investigation [17, 23, 24] on constitutive laws, this alloy exhibits cyclic strain softening to the extent of complete unloading even at room temperature. Round tensile specimens, 6.41 mm diameter with gauge length of 63.5 mm were used.

3.2. Experimental procedure

Cyclic loading and stress relaxation experiments were conducted on a model TTC-M Instron machine. The tests were controlled by means of a Motorola M6809 computer. For cyclic loading experiments, the computer was programmed to control the loading as illustrated in Figs. 1 and 2 for strain and load controlled tests, respectively. In both cases, the specimens were initially loaded to a predetermined load (or stress equal to σ_0) level. For the strain controlled experiments, the corresponding initial total strain, ε_0, was then the minimum strain while for load controlled experiments, the initial stress σ_0 was the minimum stress. Subsequently, the specimens were loaded at constant loading rate or constant cross-head speed either between the minimum and maximum total strain if strain is the controlled function (Fig. 1) or between minimum and maximum load if load is the controlled function (Fig. 2). The total strain was measured by using an Instron strain gauge extensometer. For the first few cycles the computer was programmed to record on a floppy disk the load-strain-time data at short intervals of time (about half a second). In the subsequent cycles, only the minimum and maximum strain or load were recorded. A similar procedure was adopted for the computer controlled stress relaxation experiments. The specimen was initially loaded at constant cross-head speed to a predetermined load or initial stress σ_0 reaching the initial strain ε_0. The cross-head was then stopped and the computer was programmed to control the cross-head position so that the specimen was maintained within the strain range $\varepsilon_0 \pm 50\,\mu\varepsilon$. The applied load was then continuously monitored and it was recorded an a floppy

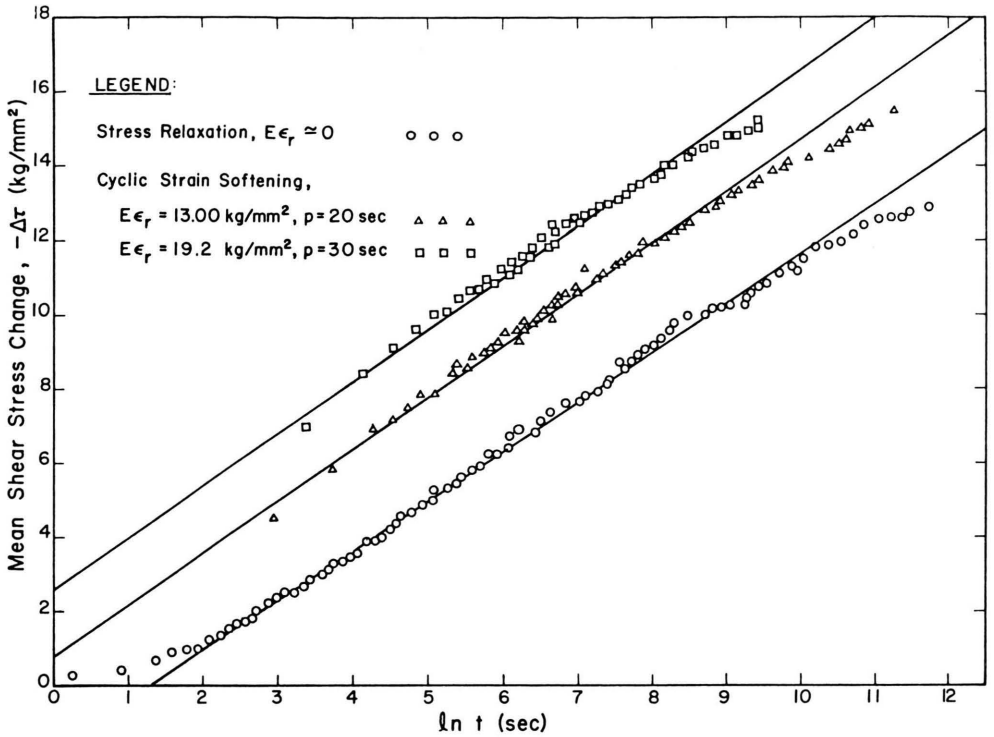

Fig. 3. Cyclic strain softening and stress relaxation mean applied shear stress change represented in the shear stress change versus natural logarithm of time coordinate system for the evaluation of activation volume. The experiments were carried out on a near eutectoid Zn-Al alloy. the experimental variables are: $\tau_0 = 15.5$ kg/mm^2, cross-head speed = 1.5 mm/min and temperature = 293 K.

disk as a function of time when the decrease in the load was 1% of the initial load. A different specimen was used for each test. The temperature of the specimen was maintained by controlling room temperature to better than $\pm$ 1.0 K.

3.3. Experimental results

3.3.1. Cyclic strain softening

The experimental results for cyclic strain softening and stress relaxation were plotted on a $-\Delta\tau$ (mean shear stress change) and logarithm of time coordinate system for the determination of the constitutive parameters [11, 16]. Typical results are presented in Figure 3. The experiments were carried out at room temperature, 293 $\pm$ 1.0 K, with an initial shear stress of 15.5 kg/mm^2. The lines were obtained from least square method using (13) (in integrated form [16]) and (14) for cyclic loading and stress relaxation, respectively. In the high stress zone, the constitutive equation of cyclic strain softening predicts a linear relationship between the mean shear stress change and the logarithm of time. The deviation of experimental points from the straight line was indeed expected from a study of deformation kinetics of the alloy [23, 24]. The kinetics analysis based on this previous study showed that the rate of plastic flow is controlled by a consecutive operation of two mechanisms (or energy barriers). In the high stress range where the plot is linear, one of the mechanisms is rate controlling while the deviation from linearity signifies that in the subsequent stress range, the other energy barrier controls the rate of plastic flow. The activation volume (inversely proportional to the slope) was $16b^3$ for stress relaxation and $15b^3$ for both cyclic strain softening experiments. The product EA_f was 7.1×10^{-6} kg/mm^2 sec for stress relaxation while for cyclic strain softening it was within $2 \sim 3 \times 10^{-6}$ kg/mm^2 s. The results are well in agreement with the observation made in our previous paper, that is, the material structural characteristics (activation

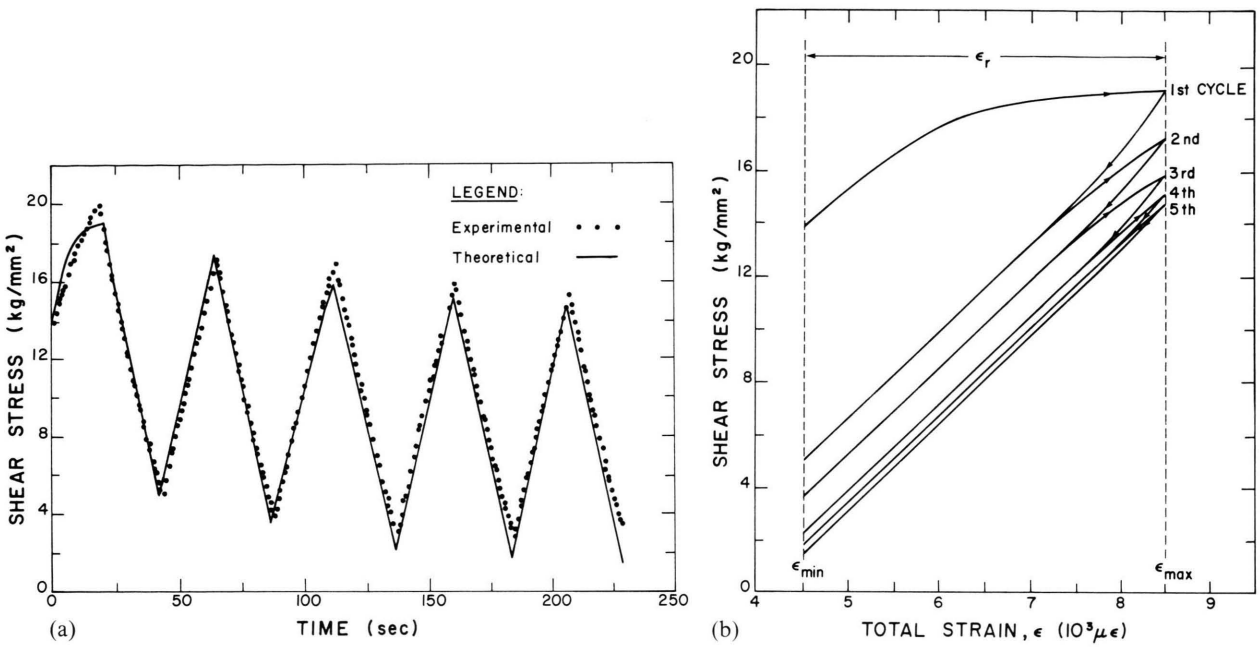

Fig. 4. Stress-time, and stress-strain response during the first few cycles of a strain controlled, cyclic loading experiment. The parameters are: $V_f = 16b^3$, temperature = 293 K, $EA_f = 7.1 \times 10^{-6}$ kg/mm^2 sec, $\tau_0 = 14$ kg/mm^2, cross-head speed = 1.0 mm/min, $E\,\varepsilon_r = 26.3$ kg/mm^2.
(a) Shear stress-time response during cyclic strain softening. The symbols represent the experimental data while the line was calculated with (13).
(b) Calculated hysteresis loops plotted on a shear stress versus total strain axes.

parameters) determined from stress relaxation and cyclic strain softening are essentially identical. The slight difference between the results from the two experiments could be due to variations in material structure, i.e. variations in the mobile dislocation density and the free energy of activation between the different specimens used. Furthermore, the assumption that the material structure remains constant during the deformation is valid only for small strain amplitudes.

Figure 4a shows the shear stress-time response during the first few cycles of a strain controlled cyclic loading (with a triangular strain wave form) experiment. The symbols represent the experimental results while the solid line was calculated from (13) using the structural characteristics determined from the results of a stress relaxation experiment. It is observed that the constitutive equation describes well the deformation behavior during cyclic strain softening. To illuminate the deformation process, the stress response was plotted on a shear stress versus total strain axes, leading to hysteresis loops as shown in Figure 4b. Each strain cycle leads to a decrease in the applied shear stress. The greater is the number of cycles the smaller is the decrease in applied shear stress per cycle. That is, within the stress, time and temperature range where the thermally activated plastic flow during cyclic strain softening can be approximated with activation over a single energy barrier, the applied shear stress is proportional to the logarithm of the time or number of cycles. In Figs. 5a and 5b, the hysteresis loops for the first and second cycles were replotted from Fig. 4b and were compared with experimental data. There is a good agreement between the calculated hysteresis loops and the experimental results. The slight deviations between the two are probably due to the large strain amplitude which may have led to increase in the mobile dislocation density.

3.3.2. Cyclic stress softening

Figure 6 shows typical experimental results for cyclic stress softening experiments that were carried out at room temperature, 293 ± 1.0 K, and for a stress amplitude of 61 MPa (6.2 kg/mm^2). Mean plastic strain (or the difference between mean total strain and mean elastic strain) was plotted as a

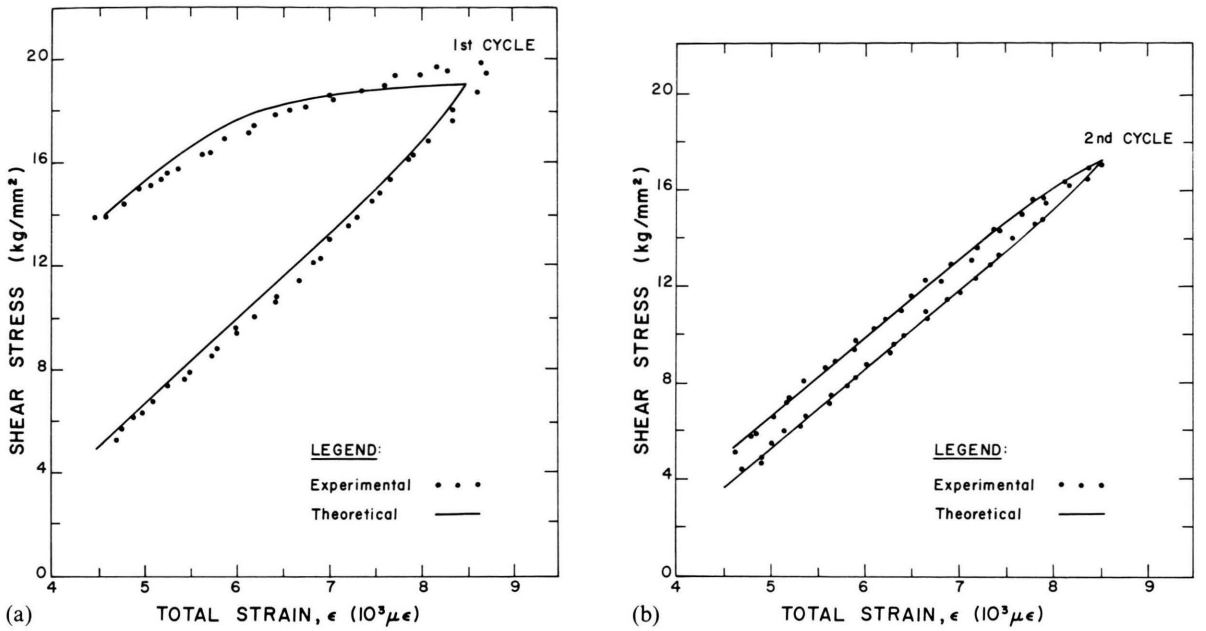

Fig. 5. Comparison of the calculated hysteresis loops (solid line) and the experimental data (symbols). The calculated hysteresis loops were replotted from Figure 4b. (a) Hysteresis loop for the first cycle. (b) Hysteresis loop for the second cycle.

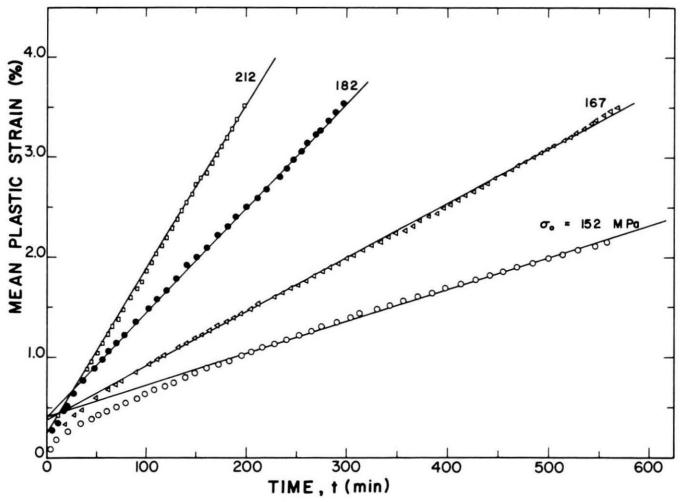

Fig. 6. Mean plastic strain plotted as a function of time for different initial stress levels. The lines were obtained from least square method using (22) while the symbols represent the measured values. The parameters are: Temperature = 293 K, $E = 6580$ kg/mm^2, $\sigma_r = 61$ MPa and Cross-head speed = 1.0 mm/min.

function of time for each initial stress level. The lines were obtained from least square method using (23). The linear time dependence indicates that no work hardening occurred: this is an indication of constant structure. The slope of each of the lines represents the mean plastic strain rate at the corresponding initial stress level. The activation parameters were analyzed by plotting the mean plastic strain rate and the initial stress on a semi-logarithm scale as shown in Figure 7. According to (23), the plot should be a straight line; the slope of which is proportional to the activation volume, V_f, while its intercept at $\sigma_0 = 0$ is proportional to the activation parameter, A_f, for a given stress amplitude. Con-

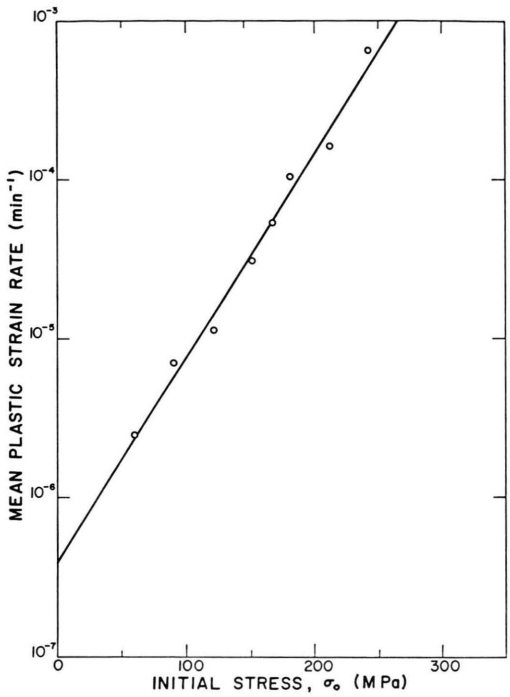

Fig. 7. The logarithm of mean plastic strain rate plotted as a function of the initial stress. The line was obtained from least square method. The circles represent the experimental data (the mean plastic strain rate is the slope of the mean plastic strain versus time plot of the respective initial level as shown in Figure 6).

sequently, the activation volume was determined as $12b^3$ and the parameter A_f was 1.16×10^{-9}/sec.

Figure 8 shows the strain versus time response during the first few cycles of a load controlled cyclic loading (with a triangular load wave form) experiment. The symbols represent the experimental results while the solid line was calculated by integrating (17) for the case where the microstructure is constant and by using the constitutive parameters determined from the results presented in Figs. 6 and 7. It is observed that the constitutive equation describes well the deformation behavior during cyclic stress softening. To visualize the deformation process, the strain response was plotted on a stress-strain coordinate system as shown in Figure 8 b. It is apparent that each load cycle leads to an increment in the strain. That is, within the stress, time and temperature range where thermally activated plastic flow in cyclic creep can be approximated with activation over a single energy barrier, the total strain is related to the number of strain cycles. It is

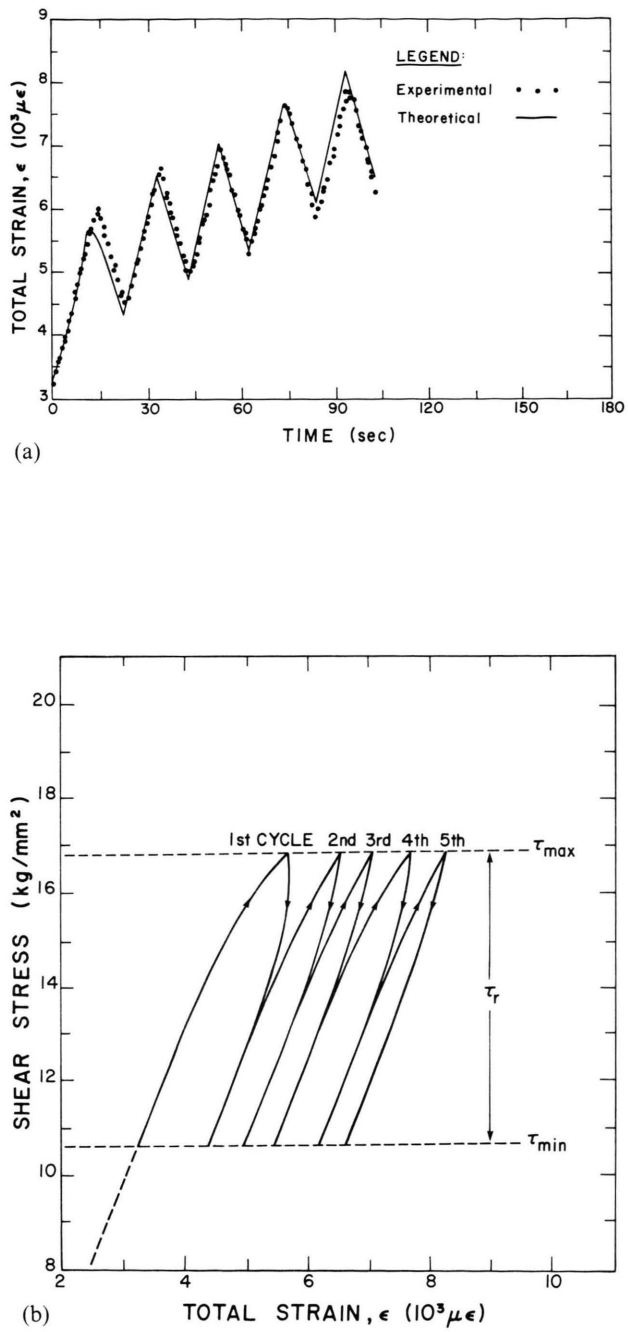

Fig. 8. Strain-time and stress-strain response during the first few cycles of a load controlled, cyclic loading experiment. The parameters are: $V_f = 12b^3$, $A_f = 1.16 \times 10^{-9}$/sec, $\sigma_0 = 21.7$ kg/mm^2, $\sigma_r = 12.4$ kg/mm^2, temperature = 293 K, $\varepsilon_0 = 3.26 \times 10^{-3}$, cross-head speed = 1.5 mm/min and $E = 6580$ kg/mm^2.
(a) Total strain-time response. The symbols represent the experimental data while the curve was calculated with (17).
(b) Calculated hysteresis loops presented on stress-strain axes.

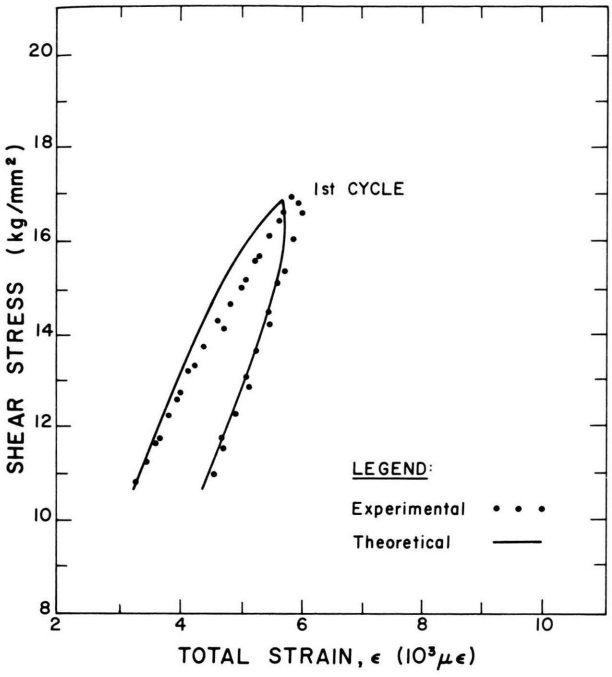

(a)

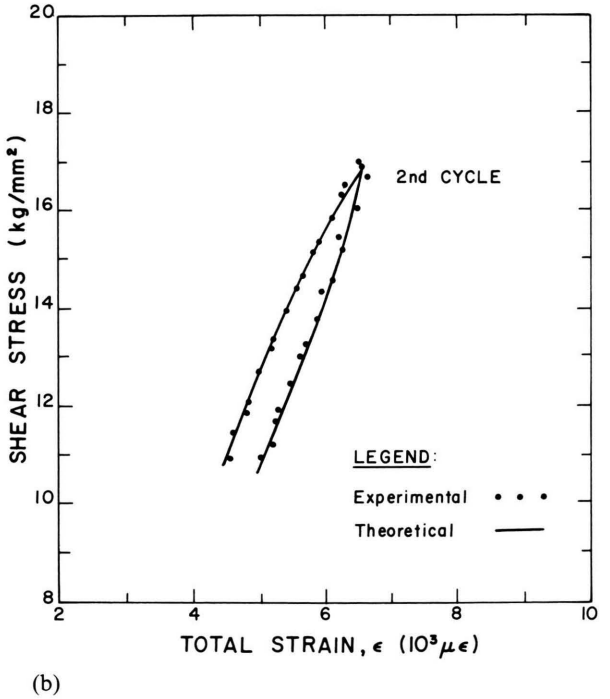

(b)

Fig. 9. comparison of the calculated hysteresis loops (solid line) and the experimental data (symbols). The calculated hysteresis loops were replotted from Fig. 8 b.
(a) Hysteresis loop for the first cycle.
(b) Hysteresis loop for the second cycle.

evident from Fig. 9 that there is a good agreement between the calculated hysteresis loops and the experimental data.

3.4. Constitutive parameters

In our previous study [16], the activation parameters for cyclic strain softening of the Zn-Al alloy were determined. It was found that the activation volume was $13 \pm 1\,b^3$ while the activation parameter A_f was within the range 7×10^{-10}/sec to 5×10^{-9}/sec. The experiments were carried out in the same stress and temperature range as the results reported in the present paper. Also, the constitutive parameters for both stress relaxation and cyclic strain softening process were found to be identical. The present analysis shows that the activation volume for cyclic stress and strain softening is $14 \pm 2\,b^3$ while the activation parameter A_f is within the range 0.3×10^{-9}/sec to 1.1×10^{-9}/sec. Clearly, therefore, the material structural characteristics (activation parameters) for cyclic stress softening, cyclic strain softening and stress relaxation are essentially identical. It seems, therefore, that cyclic stress softening and cyclic strain softening are different manifestations of the same basic process, depending on the control condition.

At high temperatures (over $0.4\,T_m$, where T_m is the melting temperature), the rate of plastic deformation of the Zn-Al alloy is controlled mainly by grain boundary sliding [26–30]. Other mechanisms contributing to the plastic flow include diffusional creep and dislocation slip and/or climb [26–30]. The rate controlling deformation mechanism(s) of the alloy at room temperature (below $0.4\,T_m$) has not been established although it is widely accepted [26–30] that dislocation movement inside the grains may be rate controlling. The measured activation volume at room temperature for cyclic strain and stress softening indicate that the process may be controlled by dislocation movement, either by Peierls-Nabarro mechanism or by cross-slip mechanism [11].

4. Conclusions

It is concluded that cyclic strain softening and cyclic stress softening of materials with low internal stress levels are rate phenomena, strongly dependent on the temperature and loading rate. Over the high

stress and low temperature range where thermally activated plastic flow in cyclic strain and stress softening can be approximated with activation over a single energy barrier, cyclic strain softening is essentially a stress relaxation process while cyclic stress softening appears to be a creep process. The material structural characteristics for cyclic strain softening, cyclic stress softening and stress relaxation are identical. It was shown that the structural characteristics determined from a simple stress relaxation test can be used to predict the cyclic softening behavior, using the constitutive equations derived in this report. However, the validity of the constitutive equations is limited to the low temperature, high stress, and time (or number of cycles) range where the rate of thermally activated plastic flow can be approximated with activation over a single energy barrier. It is also limited to cyclic deformation during which the mobile dislocation density (and hence the internal stress) remains constant. This limitation implies that the strain and stress amplitudes should be small, depending on the variation of the mobile dislocation density with stress or strain. For the Zn-Al alloy, the variation of the mobile dislocation density with the stress or strain amplitudes and with the number of cycles seems to be insignificant. At high strain rates (or high frequencies), the rate of plastic flow is limited by the velocity of transverse sound waves in the material. Nevertheless, thermally activated plastic flow ends – fades out – at strain rates several orders of magnitude below this. The extension of the theory and experimental verification to a wider stress and temperature range as well as to creep will be presented elsewhere [23].

Acknowledgements

The financial assistance by the Natural Science and Engineering Research Council of Canada and by the German Academic Exchange Service (to J. S. Mshana) are gratefully acknowledged. We appreciate helpful discussions with Prof. B. Ramaswami, Dept. of Metallurgy, University of Toronto.

Appendix

The integral $\int_0^t \exp \frac{V_f \sigma(t)}{2kT} dt$ represents the area under $f(t)$ versus t diagram where $f(t) = \exp \frac{V_f \sigma(t)}{2kT}$. The stress wave function $\sigma(t)$ is

$$\sigma(t) = \sigma_0 + \sigma_1(t) \tag{A.1}$$

where $\sigma_1(t)$ is defined for the first cycle as

$$\sigma_1(t) = \begin{cases} \frac{2\sigma_r t}{p} & \text{when} \quad 0 \leqq t \leqq \frac{p}{2}, \\ \frac{2\sigma_r}{p}(p-t) & \text{when} \quad \frac{p}{2} \leqq t \leqq p. \end{cases} \tag{A.2}$$

In (A.2), σ_r is the stress range or amplitude and p is the period as illustrated in Figure 2. Consider the first cycle where $0 \leqq t \leqq p$. The integral, I_1, is

$$I_1 = \left\{\exp \frac{V_f \sigma_0}{2kT}\right\} \int_0^p \exp \frac{V_f \sigma_1(t)}{2kT} dt = \left\{\exp \frac{V_f \sigma_0}{2kT}\right\}$$

$$\cdot \left| \int_0^{p/2} \exp \frac{V_f \sigma_r t}{kTp} dt + \int_{p/2}^{p} \exp \frac{V_f \sigma_r (p-t)}{kTp} dt \right|$$

$$= \left\{\exp \frac{V_f \sigma_0}{2kT}\right\} \left\{\frac{kTp}{V_f \sigma_r} \left| \exp \frac{V_f \sigma_r}{2kT} - 1 \right| - \frac{kTp}{V_f \sigma_r} \right.$$

$$\left. \cdot \exp \frac{V_f \sigma_r}{kT} \left| \exp - \frac{V_f \sigma_r}{kT} - \exp - \frac{V_f \sigma_r}{2kT} \right| \right\}$$

$$= \frac{2kTp}{V_f \sigma_r} \left\{\exp \frac{V_f \sigma_0}{2kT}\right\} \left| \exp \frac{V_f \sigma_r}{2kT} - 1 \right|.$$

Hence, for m cycles, $t = mp$ and the integral I_m is

$$I_m = m I_1 = \frac{2kTt}{V_f} \left\{\exp \frac{V_f \sigma_0}{2kT}\right\} \left| \frac{\exp \frac{V_f \sigma_r}{2kT} - 1}{\sigma_r} \right|. \tag{A.3}$$

[1] L. F. Coffin and Erhard Krempl, Editors, Cyclic Stress-strain Behavior – Analysis, Experimentation and Failure Prediction, ASTM, STP 519, American Society for Testing and Materials, 1973.
[2] M. Klesnil and P. Lukas, Fatigue of Metallic Materials, Elsevier Scientific Publishing Company, New York 1980.
[3] A. S. Argon, Editor, Constitutive Equations in Plasticity, MIT Press, Cambridge, Mass., 1975.
[4] R. W. Hertzberg, Deformation and Fracture Mechanics of Engineering Materials, John Wiley and Sons, New York 1976.
[5] R. M. Wetzel, A Method of Fatigue Damage Analysis, Ford Motor Company Technical Report No. SR 71-107, 1971.
[6] R. M. Wetzel, Editor, Fatigue Under Complex Loading: Analysis and Experiments, Advances in Engineering, Vol. **6**, SAE, 1977.
[7] U. F. Kocks, A. S. Argon, and M. F. Ashby, Thermodynamics and Kinetics of Slip, Pergamon Press Ltd., London 1975.
[8] Erhard Krempl, Cyclic Plasticity: Some Properties of Hysteresis Curve of Structural Metals at Room Temperature, ASME paper No. 69-WA/Met-4, 1969.
[9] A. Fox, Editor, Stress Relaxation Testing, ASTM, STP 676, American Society for Testing and Materials, 1979.
[10] A. S. Krausz and K. Krausz, A Review of Rate Dependent Plastic Deformation Processes and the Associated Constitutive Laws, C. S. Desai and R. H. Gallagher, Editors, Proceedings of the International Conference on "Constitutive Laws for Engineering Materials Theory and Application" held in Tucson, Arizona, USA, Jan. 10–14, 1983.
[11] A. S. Krausz and H. Eyring, Deformation Kinetics, Wiley-Intersci., New York 1975.
[12] H. Eyring, J. Chem. Phys. **4**, 283 (1936).
[13] E. Orowan, Proc. Roy. Soc. London **52**, 8 (1940).
[14] A. S. Krausz and B. Faucher, Energy-Barrier Systems in Thermally Activated Plastic Flow, Reviews on the Deformation Behavior of Materials, P. Feltham, Ed., **IV**, No. 2 (1982).
[15] A. S. Krausz and B. Faucher, A Kinetics Approach to the Derivation and Measurement of the Constitutive Equations of Time-dependent Deformation, Mechanical testing for Deformation Model Development, ASTM STP 765, R. W. Rhode and J. C. Swearengen, Eds., American Society for Testing and Materials, pp. 284–297 (1982).
[16] J. S. Mshana and A. S. Krausz, Constitutive Equation of Cyclic Softening, Trans. of ASME Journal of Engineering Materials and Technology, Vol. 107, No. 1, pp. 7–12 (1985).
[17] J. Mshana, A. S. Krausz, and J. Denis, An Analysis of the Constitutive Equations of Cyclic Softening, Proceedings of the 9th Canadian Congress of Applied Mechanics, Saskatoon, Canada, May 30–June 3, 1983, pp. 314–315.
[18] S. N. Komnik, J. T. Ponomarenko, and V. I. Startsev, Fiz. Metal. Metalloved **42** (No. 2), 388 (1976).
[19] J. D. Lee, P. Niessen, J. Mat. Sci. **9**, 1467 (1974).
[20] S. H. Vale, D. J. Eastgate, and P. M. Hazzledine, Scripta Met. **13** (No. 12), 1157 (1979).
[21] W. J. Cunningham, Introduction to Non-linear Analysis, McGraw-Hill Book Company, Inc., New York 1958, p. 63.
[22] W. G. Johnston, J. Appl. Phys. **33**, 2716 (1962).
[23] J. S. Mshana, Rate Dependent Constitutive Equations of Cyclic Softening and Hardening, Ph.D. Thesis under preparation, Department of Mechanical Engineering, University of Ottawa.
[24] C. H. Laforce, A. S. Krausz, and W. Ginman, The Deformation Kinetics of Near-Eutectoid Zn-Al Alloy, Z. Metallkde. **69**, 622 (1978).
[25] C. H. Laforce, The Deformation Kinetics of a Superplastic Zinc-Aluminum Alloy, M.A. Sci. Thesis, versity of Ottawa 1977.
[26] I. I. Novikov, V. K. Portnoy, and T. E. Terentieva, Acta Metallurgica **25**, 1139 (1977).
[27] A. Arieli and A. K. Mukherjee, Acta Metallurgica **28**, 1571 (1980).
[28] P. Chaudhari, Acta Metallurgica **15**, 1777 (1967).
[29] M. L. Vaidya, K. Linga Murty, and J. E. Dorn, Acta Metallurgica **21**, 1615 (1973).
[30] Farghalli, A. Mohamed, Shen-Ann Shei, and Terence G. Langdon, Acta Metallurgica **23**, 1443 (1975).